Journal of Solid Mechanics Vol. 13, No. 4 (2021) pp. 460-484
DOI: 10.22034/jsm.2021.1912143.1650

Nonlinear Investigation of Magnetic Influence on Dynamic Behaviour of Non-Homogeneous Varying Thickness Circular Plates Resting on Elastic Foundations

S.A. Salawu [1,*], G.M. Sobamowo [2], O.M. Sadiq[1]

[1]*Department of civil and Environmental Engineering, University of Lagos, Akoka, Nigeria*
[2]*Department of Mechanical Engineering, University of Lagos, Akoka, Lagos, Nigeria*

Received 30 July 2021; accepted 5 October 2021

ABSTRACT

In this work, a nonlinear investigation of non-homogeneous varying thickness circular plates resting on elastic foundations under the influence of the magnetic field is investigated. The non-homogeneity of the circular plates' material is presumed to occur due to linear and parabolic changes in Young's modulus likewise the density along the radial direction in a unique manner. The geometric Von Kármán equations are used in modelling the governing differential equations. The transverse deflection is approximated using an assumed single term mode shape while the central deflection in form of Duffing's equation is obtained using the Galerkin method. Subsequently, the semi-analytical solutions are provided using the Optimal Homotopy Asymptotic Method (OHAM), the analytical solutions are used for parametric investigation. The results in this work are in good harmony with past results in the literature. From the results, it is realized that the nonlinear frequency of the circular plate increases with an increase in the linear elastic foundation. Also, the results showed that clamped edge and simply supported edge condition produced the same hardening nonlinearity. However, varying taper and non-homogeneity lower the nonlinear frequency ratio. Also, maximum deflection occurs when excitation force is zero, and attenuation of deflection is observed due to the presence of a magnetic field, varying thickness, homogeneity, and elastic foundation. It is anticipated that the discoveries from this research will boost the design of structures subjected to vibration.

Keywords : Nonlinear vibration; Non-homogeneous; Variable thickness circular plates; Three-parameter foundations; Optimal homotopy asymptotic method.

1 INTRODUCTION

WITH the advent of modern science and technology, structures under magnetic field usage in different fields

[*]Corresponding author. Tel.: +23 48034306342.
E-mail address: 129042077@live.unilag.edu.ng (S.A. Salawu)

of industry have been intensified. Consequently, higher demands for the design of modern machinery are put forward, that is, the dynamic feature of the structure should be fully considered in the structure design process. Thus, it is very germane to scrutinize the dynamic behavior of such plates under the effect of external force to avoid resonance. Many authors had worked on nonlinear vibration of variable thickness plates. In the problem of the dynamic behavior of plates under an in-plane force, Zhiming [1] analyzed the nonlinear vibration of exponential varying thickness circular plates using Galerkin and Perturbation method. The influence of the thickness variation was considered and it was found out that, increasing the thickness increases the nonlinear natural frequency. In another study, Wattanasakulpong and Charoensuk [2] obtained solutions for the vibration of stepped beams comprised of functionally graded material (FGM) plates using the Differential Transformation Method. The author obtained the differential governing equation using Hamilton's principle. It was detected that the value of natural frequencies increases with foundation stiffness increment. In another work, Chakravorty [3] investigated the bending and buckling of the annular hole circular plate of variable thickness under symmetric loading using the exact method. It was found out that, no buckling in the presumed finite body deflection of the annular plate. Hu and Wang [4] worked on a circular plate under the magnetic field. Also, [5] obtained buckling loads through analytical methods. There are sizeable numbers of publications on the analysis of FGM plates under external loading. [6] analyzed plate vibration based on classical and shear order deformation plate theories using an analytical method for free vibration. Results obtained show that buckling mode numbers fluctuate with power-law index variation. In a later work, Shishesaz *et al.* [7] used a GDQ method for the investigation of magneto-elastic analysis of annular FGM plates. Banerjee [8] studied large deflection of clamped edge circular plates using Dutta and Banerjee equations. Based on the results, the increase in values of thickness the deflection of the circular plate increases for clamped edge condition. In another study, Shariyat *et al.* [9] adopted the principle of complex modulus laterally on an elastic-viscoelastic plate while the power series solution is used to obtain the solution. It was realized that an increase in thickness, foundation stiffness, and material loss factor leads to higher natural frequencies. For real-life problems, the adoption of two-parameter foundations predicts a better result than only Winkler elastic foundation because of the provision for cohesion among the spring elements. The present research adopts three-parameter foundations and is peculiar to the railway track. To investigate the response of plates resting on elastic foundations, Gupta *et al.* [10] studied the free vibration response of non-homogenous, variable thickness rectangular on elastic foundation using the Differential Quadrature Method. The authors employed classical plate theory for the formulation of the governing equation. Also, Malekzadeh [11] adopted the GDQ method to analyze FGM plates placed on elastic foundations. In this study, geometric Von Kármán nonlinear equations are used to cater for nonlinear strain in the governing equation. This condition is of greater importance when the plate is subjected to the vibration amplitude of the equal order of the plate thickness. There is a huge number of pieces of literature concerning plate theories and plate dynamics. Meanwhile, Kamal and Durvasula [12] used Chebyshev polynomial using the Lanczos technique (analytical method) to investigate circular plate bending resting on an elastic foundation. Yazdi [13] employed the Homotopy perturbation method (HPM) to determine the deflection and frequency ratio of circular plates on three-parameter foundations. It was observed that increasing the elastic foundation parameters and orthotropic parameter value results in a decrease frequency ratio. [14,15] used the Ritz method in analyzing free vibration of varying thickness and non-homogenous plates. In another work, [16,17] investigated the dynamic analysis of plate resting on the three-parameter foundation. Touze *et al.* [18] studied nonlinear examination of circular plates using the Von Kármán principle. Khalsa [19,20] investigated thermoelastic large deflection bending analysis of elliptical plate resting on elastic foundations. In another work, [21-25] studied dynamic behaviour of nanoplates. Findings had shown that nonlinear problems are not easy to analyze. This is because of the complexity introduced as a direct result of a nonlinear variable, thereby limiting the choice of methods that may be adopted to obtain accurate solutions. The use of numerical solutions requires stability and convergence studies which increase the computation time and cost. More so, the exact method requires a sound knowledge of mathematics coupled with the challenges of handling nonlinear problems. Semi-analytical methods are highly effective in handling nonlinear problems. Some of them are associated with few challenges. GDQ and Power series methods also have limitations of defining valid function and divergence of series solutions. Galerkin and Perturbation method also requires finding insignificant perturbation parameters. The difficulty of obtaining Chebyshev polynomial is also a limitation. The need for a symbolic solution prompts the use of the semi-analytical method. [13,26] considered the use of the HPM for the analysis of circular plates. Zhong [27] applied HAM in obtaining a solution for the Von Karman plate. Though HPM and HAM are reliable method of solution for the nonlinear problem but suffers the setback of embedded parameters and initial solution with direct implication on timing and cost of the computation. OHAM is by far a more effective method for solving a strongly nonlinear problem, easy to use, versatile and improvement on HPM. The edge OHAM has over other semi-analytical methods justifies the choice for this study.

The previous investigations into the nonlinear analysis of non-homogeneous varying thickness circular plates on elastic foundations as reviewed above have shown that a study of nonlinear vibration analysis of variable thickness circular plate under magnetic field resting on three-parameter elastic foundations using OHAM has not been investigated. Therefore, the present study concentrates on the dynamic analysis of non-homogeneous varying thickness circular plates placed on three-parameter elastic foundations under the impact of the magnetic field using the OHAM. Part of the novelties of this study is the consideration of various variations in thickness, homogeneity, and density under magnetic field. Parametric studies also conducted using the analytical solution obtained.

2 PROPLEM FORMULATION AND MATHEMATICAL ANALYSIS

Considering a nonhomogeneous, linearly varying circular plate under the impact of magnetic field resting on three-parameter foundations as illustrated in Fig. 1. The circular plate is resting on a linear, nonlinear Winkler and Pasternak foundation. The governing equations as reported by [13,26, 28] are:

$$\begin{aligned} &D\frac{\partial}{\partial r}\left\{r\frac{\partial}{\partial r}\left[\frac{1}{r}\frac{\partial}{\partial r}\left(r\frac{\partial w}{\partial r}\right)\right]\right\}+k_w w-k_s\nabla^2 w+k_p w^3-\frac{1}{r}\frac{\partial}{\partial r}\left(f\frac{\partial w}{\partial r}\right)-\frac{h^3}{12}Boz\left(\frac{1}{r}\frac{\partial^2 w}{\partial r^2}+\frac{\partial^3 w}{\partial r^2\partial t}\right)\\ &=Q_0\cos(\omega t)-\rho h\frac{\partial^2 w}{\partial t^2}-\left(r\frac{\partial^2 w}{\partial r^2}+\nu\frac{\partial w}{\partial r}\right)\frac{\partial^2 D}{\partial r^2}-\left[2r\frac{\partial^3 w}{\partial r^3}+(2+\nu)\frac{\partial^2 w}{\partial r^2}-\frac{1}{r}\frac{\partial w}{\partial r}\right]\frac{\partial D}{\partial r}\end{aligned} \tag{1}$$

$$\frac{\partial^2 f}{\partial r^2}+\frac{1}{r}\frac{\partial f}{\partial r}-\frac{f}{r^2}+\frac{E}{2r}\left(\frac{\partial w}{\partial r}\right)^2=0, \tag{2}$$

where t is the time, r is the radial coordinate, w is the transverse deflection, E is Young's modulus of the plate. The Winkler foundation is k_w , k_s is the Pasternak foundation, k_p the nonlinear Winkler. Q_0 is the uniformly distributed transverse load, ω is the excitation frequency while ρ is the material density, h is the plate thickness, flexural rigidity $D=Eh^3/12(1-\nu^2)$, Boz is the external magnetic field, f is the Airy stress and Poisson's ratio is v. Using dimensionless parameters

$$\begin{aligned} &F=\frac{f}{D^*},W=\frac{w}{h},R=\frac{r}{a},K_s=\frac{k_s a^2}{D^*},K_w=\frac{k_w a^4}{D^*},K_p=\frac{k_p a^4}{D^*},Q=\frac{Q_0 a^4}{D^*},\\ &\frac{\partial^2 F}{\partial R^2}+\frac{1}{R}\frac{\partial F}{\partial R}-\frac{F}{R^2}+\frac{g(R)}{2R}\frac{E}{D_0}\left(\frac{\partial W}{\partial R}\right)^2=0,\end{aligned} \tag{3}$$

$$\begin{aligned} &g(R)^3\frac{\partial^4 W}{\partial R^4}+2\left[\frac{g(R)^3}{R}+R\frac{\partial g(R)^3}{\partial R}\right]\frac{\partial^3 W}{\partial R^3}+\left[-\frac{g(R)^3}{R^2}+(2+\nu)\frac{\partial g(R)^3}{\partial R}+R\frac{\partial^2 g(R)^3}{\partial R^2}\right]\frac{\partial^2 W}{\partial R^2}\\ &+\left[\frac{g(R)^3}{R^3}-\frac{1}{R}\frac{\partial g(R)^3}{\partial R}+\nu\frac{\partial^2 g(R)^3}{\partial R^2}\right]\frac{\partial W}{\partial R}-K_s\frac{\partial^2 W}{\partial R^2}+\frac{K_s}{R}\frac{\partial W}{\partial R}+K_w W+K_p W^3\\ &+\frac{1}{R}\left(F\frac{\partial^2 W}{\partial R^2}\right)-\frac{1}{R}\left(\frac{\partial F}{\partial R}\frac{\partial W}{\partial R}\right)-\frac{g(R)^3}{12}Boz\left(\frac{1}{R}\frac{\partial^2 W}{\partial R^2}+\frac{\partial^3 W}{\partial R^2\partial t}\right)=-\frac{\rho a^4 g(R)}{D_0}\frac{\partial^2 W}{\partial t^2}+Q_0\cos(\omega t),\end{aligned} \tag{4}$$

Assuming $\mu=Eh_m^3/12(1-\nu^2)$, then, $D=\mu\left[g(R)\right]^3$. Two variation cases considered are:

- Linear variation of plate thickness, non-homogeneity of plate material variation in the radial direction. The thickness h of the plate at an arbitrary point is anticipated to be $h(R)=h_0(1+\gamma R)$, the non-homogeneity parameter is $\rho=\rho_0(1+\alpha R), E=E_0(1+\eta R)$ and $K_w=K_0(1-\varepsilon R),\ 0\le\varepsilon\le 1$.

Therefore, $D = \mu\left[1+3\gamma R+3\gamma^2 R^2+\gamma^3 R^3\right]$

- Parabolic variation of plate thickness, non-homogeneity of plate material in the radial direction.

Parabolic thickness $h(R)=h_0(1+\gamma R^2)$, the non-homogeneity parameter is $\rho=\rho_0(1+\alpha R^2), E=E_0(1+\eta R^2)$, and $K_w=K_0(1-\varepsilon R^2),\ 0\le\varepsilon\le 1$. Where h_0,ρ_0,E_0,K_0 are the thickness of the plate, density, Young modulus of the plate material at the middle of the plate, and Winkler foundation parameter, respectively. While $\gamma,\alpha,\eta,\varepsilon$ are the taper parameter, non-homogeneity, and Winkler constant parameters at $R=\alpha$ respectively. $D_0=\dfrac{E_0h_0^3}{12(1-\nu^2)}$, where

$$D = D_0 \times g(R), \tag{5}$$

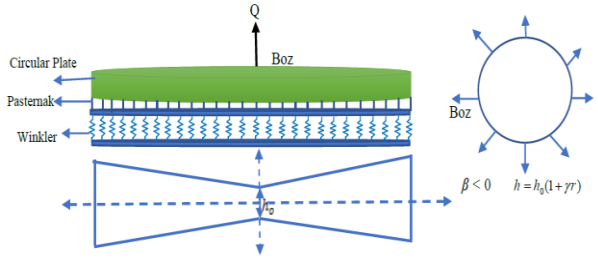

Fig.1
Showing varying thickness circular plate on three-parameter foundations.

Figs. 2-5 show some industrial applications of the problem under consideration.

Fig.2
Train moving on the railway track.Source: Google search.

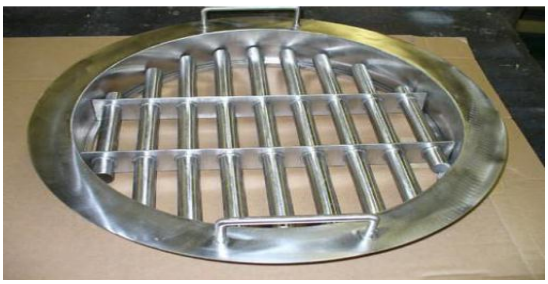

Fig.3
Circular Magnetic grill cover. Source: Google search.

Fig.4
Circular magnetic object lifter. Source: Google search.

Fig.5
Automobile brake system. Source: Google search.

3 METHOD OF SOLUTION

An approximate solution is obtained by assuming the non-linear vibrations to have the same spatial shape, i.e.,

$$W(r,\tau)=\left(c_4 r^4+c_2 r^2+1\right)\varphi(t) \tag{6}$$

Substitute Eq. (6) into Eq. (3) and solve the ODE

$$F=\frac{c_1}{r}+rc_3-\frac{\left(\varphi(t)\right)^2 h_o r^3\begin{pmatrix}126c_4{}^2\eta\gamma r^6+210c_2c_4\eta\gamma r^4+160c_4{}^2r^5\eta+160c_4{}^2\gamma r^5+105c_2{}^2\eta\gamma r^2+\\ 288c_2c_4r^3\eta+288c_2c_4\gamma r^3+210c_4{}^2r^4+168c_2{}^2r\eta+168c_2{}^2\gamma r+\\ 420c_2c_4r^2+315c_2{}^2\end{pmatrix}}{1260D_o}, \tag{7}$$

The value F is accordingly found to be finite at the origin $c_1=0$. Additionally, c_3 is the integration constant to be determined from in-plane boundary conditions. The Substitution of the expressions for W and F given by Eqs. (6) and (7) respectively into Eq. (4) and the application of the Galerkin procedure in the nonlinear time differential equation obtained in the form

$$\int_0^1 L'(w,F)w\ \ r\ dr=0 \tag{8}$$

where

$$\begin{aligned}
&L'=\left(\gamma^3R^3+3\gamma^2R^2+3\gamma R+1\right)(1+\eta R)\frac{\partial^4W}{\partial R^4}+2\left[\frac{\left(\gamma^3R^3+3\gamma^2R^2+3\gamma R+1\right)(1+\eta R)}{R}+\right.\\
&\left.R\left(3\gamma^3R^2+6\gamma^2R+3\gamma\right)(1+\eta R)\right]\frac{\partial^3W}{\partial R^3}+\\
&\left[-\frac{\left(\gamma^3R^3+3\gamma^2R^2+3\gamma R+1\right)(1+\eta R)}{R^2}+(2+\nu)\left(3\gamma^3R^2+6\gamma^2R+3\gamma\right)(1+\eta R)+\right.\\
&\left.R\left(6\gamma^3R+6\gamma^2\right)(1+\eta R)\right]\frac{\partial^2W}{\partial R^2}+\\
&\left[\frac{\left(\gamma^3R^3+3\gamma^2R^2+3\gamma R+1\right)(1+\eta R)}{R^3}-\frac{\left(3\gamma^3R^2+6\gamma^2R+3\gamma\right)(1+\eta R)}{R}\right.\\
&\left.+\nu\left(6\gamma^3R+6\gamma^2\right)(1+\eta R)\right]\frac{\partial W}{\partial R}-K_s\frac{\partial^2W}{\partial R^2}+\\
&\frac{K_s}{R}\frac{\partial W}{\partial R}+K_wW+K_pW^3+\frac{a}{R}\left(F\frac{\partial^2W}{\partial R^2}\right)-\frac{a}{R}\left(\frac{\partial F}{\partial R}\frac{\partial W}{\partial R}\right)-\\
&\frac{a\left(\gamma^3R^3+3\gamma^2R^2+3\gamma R+1\right)}{12}Boz\left(\frac{1}{R}\frac{\partial^2W}{\partial R^2}+\frac{\partial^3W}{\partial R^2\partial t}\right)=-\frac{\rho_c a^4h_o(\alpha R+1)(\gamma R+1)}{D_o}\frac{\partial^2W}{\partial t^2}+Q_0\cos(\omega t),
\end{aligned} \tag{9}$$

We have

$$M\ddot{\varphi}_s(t)+G\dot{\varphi}_s(t)+K\varphi_s(t)-V\varphi_s^3(t)=Q\cos\omega t, \tag{10}$$

where the coefficients of the duffing equation are expressed for Linear Variation as;

$$M=\frac{a^4h_o\rho_c}{12D_o}\begin{pmatrix}\left(\left(\alpha+12/11\right)\gamma+12\alpha/11+6/5\right)c_4{}^2+\\ \left(\left(\left(12\alpha/5+8/3\right)c_2+3\alpha+24/7\right)\gamma+\left(8/3\alpha+3\right)c_2+24\alpha/7+4\right)c_4\\ +\left(\left(3/2\alpha+12/7\right)c_2{}^2+\left(4\alpha+24/5\right)c_2+3\alpha+4\right)\gamma\\ +\left(12\alpha/7+2\right)c_2{}^2+\left(24\alpha/5+6\right)c_2+4\alpha+6\end{pmatrix}, \tag{11}$$

$$G=-\frac{aBoz}{11D_o}\begin{pmatrix}\left(\gamma^3+33\gamma^2/10+11/3\gamma+11/8\right)c_4{}^2+\begin{pmatrix}\left(77c_2/54+11/7\right)\gamma^3+\left(77c_2/16+11/2\right)\gamma^2\\ +\left(11/2c_2+33/5\right)\gamma+77c_2/36+11/4\end{pmatrix}c_4\\ +\frac{11c_2}{42}\left(\left(c_2+7/5\right)\gamma^3+\left(7/2c_2+21/4\right)\gamma^2+\left(21c_2/5+7\right)\gamma+7/4c_2+7/2\right)\end{pmatrix}, \tag{12}$$

$$Q=-\frac{Q_0}{6}\left(c_4+\frac{3c_2}{2}+3\right), \tag{13}$$

$$V=\frac{\begin{array}{l}34054020\left(ah_o\left(640/567+\eta\right)\gamma+640ah_o/567\left(9/8+\eta\right)+10k_pD_o/27\right)c_4^4+\\ 34054020\begin{pmatrix}200ah_o\gamma/63\left(\left(\eta+1112/975\right)c_2+21\eta/50+16/33\right)+\\ \begin{pmatrix}8896ah_o/2457\left(5005/4448+\eta\right)\\ +5/3k_pD_o\end{pmatrix}c_2+\left(16h_o/9+3200h_o\eta/2079\right)a\\ +40k_pD_o/21\end{pmatrix}c_4^3+\cdots\end{array}}{227026800D_o}, \tag{14}$$

$$K=\frac{\begin{array}{l}\left(34054020\left(-2/3aBoz+400D_o/11\left(\left(\nu+433/75\right)\eta+11\nu/10+8591/1350\right)\right)\gamma^3\right.\\ +\left(-20aBoz/9+64D_o\left(\left(\nu+65/9\right)\eta+10\nu/9+145/18\right)\right)\gamma^2\\ +\left(-5/2aBoz+80D_o/3\left(\nu+35/3\right)\eta+9\nu/8+741/56\right)\gamma+\left(-20Boz/21+20D_oc_3/3\right)a\\ -20D_o/3\left(k_s-k_w/10-64\eta/7-32/3\right)c_4{}^2\\ +34054020\begin{pmatrix}-35aBoz/36\\ +520D_o/9\left(\left(\nu+61/13\right)\eta+9\nu/8+3855/728\right)\end{pmatrix}c_2\\ -10aBoz/9+400D_o/7\left(\left(\nu+263/45\right)\eta+7/6\nu+343/50\right)\gamma^3\\ +\begin{pmatrix}\left(-10/3aBoz+100D_o\left(\left(\nu+211/35\right)\eta+8\nu/7+104/15\right)\right)c_2\\ -4aBoz+320D_o/3\left(\left(\nu+37/5\right)\eta+6/5\nu+9\right)\end{pmatrix}\gamma^2+\ldots\end{array}}{227026800D_o} \tag{15}$$

Also, the coefficients of the duffing equation are expressed for Parabolic Variation as:

$$M=\frac{h_o\,\rho_c\,a^4}{14D_o}\left(\begin{array}{l}\left(\left(\left(\left(7/3\alpha+\frac{14}{5}\right)c_2+\frac{14\alpha}{5}+7/2\right)\gamma+\left(\frac{14\alpha}{5}+7/2\right)c_2+7/2\alpha+14/3\right)c_4\\+\left(\left(7/5\alpha+7/4\right){c_2}^2+\left(7/2\alpha+14/3\right)c_2+7/3\alpha+7/2\right)\gamma+\\\left(\left(\alpha+7/6\right)\gamma+7/6\alpha+7/5\right){c_4}^2+\left(7/4\alpha+7/3\right){c_2}^2+\left(14/3\alpha+7\right)c_2+\\7/2\alpha+7\end{array}\right),\tag{16}$$

$$G=-\frac{aBoz}{14D_o}\left(\begin{array}{l}\left(\gamma^3+7/2\gamma^2+\frac{21\gamma}{5}+7/4\right){c_4}^2+\left(\begin{array}{l}\left(\frac{49c_2}{36}+7/5\right)\gamma^3+\left(\frac{49c_2}{10}+\frac{21}{4}\right)\gamma^2\\+\left(\frac{49c_2}{8}+7\right)\gamma+\frac{49c_2}{18}+7/2\end{array}\right)c_4\\+\frac{7c_2}{30}\left(\left(c_2+5/4\right)\gamma^3+\left(\frac{15c_2}{4}+5\right)\gamma^2+\left(5c_2+15/2\right)\gamma+5/2c_2+5\right)\end{array}\right),\tag{17}$$

$$\begin{aligned}V=&\frac{1}{10810800D_o}\left(1281280\left(ah_o\left(\frac{81}{64}+\eta\right)\gamma+\frac{81ah_o}{64}\left(\eta+\frac{80}{63}\right)+\frac{15k_pD_o}{32}\right){c_4}^4\right)+\\&1281280\left(\begin{array}{l}\frac{99ah_o\gamma}{32}\left(\left(\eta+\frac{100}{77}\right)c_2+\frac{32\eta}{77}+\frac{6}{11}\right)+\left(\frac{225ah_o}{56}\left(\frac{77}{60}+\eta\right)+\frac{135k_pD_o}{64}\right)c_2\\+\left(\frac{\left(27\eta+36\right)h_oa}{16}+\frac{135k_pD_o}{56}\right){c_4}^3\end{array}\right)+\cdots,\end{aligned}\tag{18}$$

$$K=\frac{1}{10810800D_o}\left(1281280\left(\begin{array}{l}\left(-\frac{135aBoz}{208}+108D_o\left(\left(\nu+\frac{61}{14}\right)\eta+\frac{15\nu}{13}+\frac{785}{156}\right)\right)\gamma^3+\\\left(-\frac{405aBoz}{176}+\frac{2430D_o}{13}\left(\left(\nu+\frac{91}{18}\right)\eta+\frac{13\nu}{11}+\frac{988}{165}\right)\right)\gamma^2+\\\left(-\frac{45aBoz}{16}+\frac{810D_o}{11}\left(\left(\nu+\frac{36}{5}\right)\eta+\frac{11\nu}{9}+\frac{319}{36}\right)\right)\gamma+\\\left(\frac{135c_3D_o}{16}-\frac{135Boz}{112}\right)a-\frac{135D_o}{16}\left(-\frac{32}{3}+k_s-k_w\ /10-8\eta\right)\end{array}\right){c_4}^2+\right)+\cdots,\tag{19}$$

$$\mathrm{Q}=\mathrm{Q}_0\left(-\frac{c_4}{6}-\frac{c_2}{4}-\frac{1}{2}\right),\tag{20}$$

3.1.1 Boundary condition

The initial and boundary conditions are

$$\varphi(0,r)=a,\ \dot{\varphi}(0,r)=0,\tag{21}$$

The boundary conditions considered for plates with outer edge elastically restrained, coupled with rotational then in-plane stiffnesses k_b^* and k_i^*, exposed to an outer edge in-plane radial force N^* are:

$$r=a:\ M_r=k_b^*\frac{\partial w^*}{\partial r},\quad N_r=N^*-k_i^*u^*,\tag{22}$$

where u^* is the radial displacement at the midplane. Introduce dimensionless parameters k_b, k_i and N

$$k_b = \frac{12k_b^* a}{Eh^3},\quad N = \left(\frac{N^*}{Eh}\right)\left(\frac{a}{h}\right)^2,\quad k_i = \frac{k_i^* a}{Eh}, \tag{23}$$

The dimensionless boundary conditions are

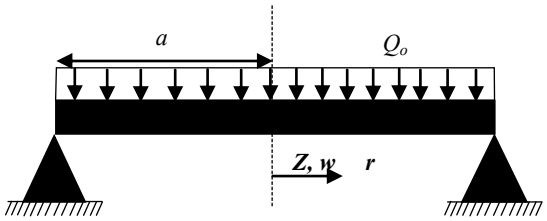

Fig.6
Schematic of a simply supported condition.

$$R = 1: \qquad W = 0, \tag{24}$$

$$\left[(1-\nu^2)k_b + \nu\right]\frac{\partial W}{\partial R} + \frac{\partial^2 W}{\partial R^2} = 0, \tag{25}$$

$$k_i\left(\frac{\partial^2 F}{\partial R^2} - \nu\frac{\partial F}{\partial R}\right) + \frac{\partial F}{\partial R} = N, \tag{26}$$

Eqs. (23) and (24) are used to find constants c_2 and c_4 while the constant of integration c_3 is obtained using Eq. (26)

$$c_2 = -\frac{2(k_b\nu^2 - k_b - \nu - 3)}{k_b\nu^2 - k_b - \nu - 5}, \qquad c_4 = \frac{k_b\nu^2 - k_b - \nu - 1}{k_b\nu^2 - k_b - \nu - 5}, \tag{27}$$

$$\begin{aligned} c_3 = -\frac{}{}\Big(& -525c_2^2\eta\gamma h_o k_i\nu - 1470c_2c_4\eta\gamma h_o k_i\nu - 1134c_4^2\eta\gamma h_o k_i\nu + 2100c_2^2\eta\gamma h_o k_i - 672c_2^2\eta h_o k_i\nu \\ & -672c_2^2\gamma h_o k_i\nu + 8820c_2c_4\eta\gamma h_o k_i - 1728c_2c_4\eta h_o k_i\nu - 1728c_2c_4\gamma h_o k_i\nu + 9072c_4^2\eta\gamma h_o k_i \\ & -1280c_4^2\eta h_o k_i\nu - 1280c_4^2\gamma h_o k_i\nu + 525c_2^2\eta\gamma h_o + 2016c_2^2\eta h_o k_i + 2016c_2^2\gamma h_o k_i - 945c_2^2 h_o k_i\nu \\ & +1470c_2c_4\eta\gamma h_o + 8640c_2c_4\eta h_o k_i + 8640c_2c_4\gamma h_o k_i - 2100c_2c_4 h_o k_i\nu + 1134c_4^2\eta\gamma h_o + \\ & 8960c_4^2\eta h_o k_i + 8960c_4^2\gamma h_o k_i - 1470c_4^2 h_o k_i\nu + 672c_2^2\eta h_o + 672c_2^2\gamma h_o + 1890c_2^2 h_o k_i + \\ & 1728c_2c_4\eta h_o + 1728c_2c_4\gamma h_o + 8400c_2c_4 h_o k_i + 1280c_4^2\eta h_o + 1280c_4^2\gamma h_o + 8820c_4^2 h_o k_i + \\ & 945c_2^2 h_o + 2100c_2c_4 h_o + 1470c_4^2 h_o + 1260ND_o \Big) \\ & \hline \\ & 1260D_o\left(k_i\nu - 1\right) \end{aligned}, \tag{28}$$

Similarly, for the Clamped condition.

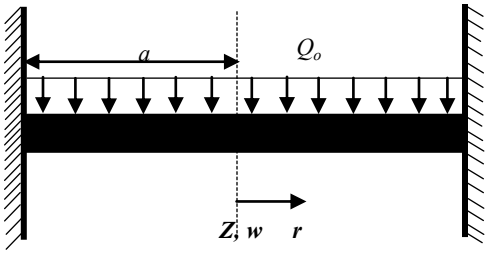

Fig.7
Schematic of a clamped-clamped supported condition.

$$W^{*}=\frac{\partial W}{\partial R}=0 \qquad c_2=-2,\ c_4=1 \tag{29}$$

3.1.2 Description of optimal homotopy asymptotic method

To illustrate the operating principle, the following general nonlinear governing equation of the form is assumed.

$$L(\varphi_s(t)+g(t)+N(\varphi_s(t)))=0, \qquad t\in\Omega, \qquad B\left(\varphi_s(t),\frac{d\varphi_s(t)}{dt}\right)=0, \quad r\in\partial\Omega, \tag{30}$$

where L is the linear operator, t signifies the independent variable, $\varphi_s(t)$ is the unknown function, N denotes the nonlinear operator, Ω is the domain, B represents the boundary operator, and $\partial\Omega$ depicts the boundary of the domain. By means of OHAM [29,30]

$$\begin{aligned}&(1-p)\left[L(\phi(t,p))+g(t)\right]=H(p)\left[L(\phi(t,p)+g(t)+N(\phi(t,p))\right],\\&B\left(\phi(t,p),\ \frac{\partial\phi(t,p)}{\partial t}\right)=0,\end{aligned} \tag{31}$$

where $p\in[0,1]$ is an embedding operator, $H(p)$ is a nonzero auxiliary function $p\neq 0$, and $\phi(t,p)$ is an unknown function when $p=0$ and $p=1$, it holds $\phi(t,0)=\varphi_0(t)$ and $\phi(t,1)=\varphi(t)$. Therefore, p it varies from 0 to 1 while it $\varphi_0(t)$ is obtained from Eq. (31) for $p=0$

3.1.2.1 Zero-order deformation

$$L(\varphi_0(t)+g(t))=0, \quad B\left(\varphi_0,\frac{d\varphi_0}{dt}\right)=0 \tag{32}$$

The auxiliary function $H(p)$ in the form

$$H(p)=pC_1+p^2C_2+\cdots \tag{33}$$

where C_1 and C_2 are constants. By expanding the Taylor series of $\phi(t,p,C_1)$ about p, we obtain

$$\phi(t,p,C_1)=\varphi_0(t)+\sum_{k=1}^{\infty}\varphi_k(t,C_1,\mathrm{C}_2,\ldots,\mathrm{C}_k)p^k \tag{34}$$

Now substituting Eq. (34) in Eq. (31) and equating the equal powers of p, we obtain the following equations:

3.1.2.2 The first and second-order problems are as follows

$$L(\varphi_1(t)+g(t))=C_1N_0(\varphi_0(t)), \quad B\left(\varphi_1,\frac{d\varphi_1(t)}{dt}\right)=0 \tag{35}$$

$$L(\varphi_2(t)-L(\varphi_1(t))=C_2N_0(\varphi_0(t))+C_1\left[L(\varphi_1(t))+N_1(\varphi_0(t)\varphi_1(t))\right], \quad B\left(\varphi_2,\frac{d\varphi_2}{dt}\right)=0 \tag{36}$$

The general governing equations $\varphi_k(t)$ are given by;

$$L(\varphi_k(t)) - L(\varphi_{k-1}(t)) = C_k N_0(\varphi_0(t) + \sum_{j=1}^{k-1} C_j \left[L(\varphi_{k-j}(t)) + N_{k-j}(\varphi_0(t), \varphi_1(t), \ldots \varphi_{k-1}(t)) \right]$$
$$B\left(\varphi_k, \frac{d\varphi_k}{dt} \right) = 0, \tag{37}$$

where $k = 2, 3, \ldots$ $N_m(\varphi_0(t), \varphi_1(t), \ldots, \varphi_{k-j}(t)$ the coefficient of p^m the expansion of $N(\phi(t, p, C_i))$ about the embedding parameter p.

$$N(\phi(t, p, C_1)) = N_0(\varphi_0(t)) + \sum_{m=1}^{\infty} N_m(\varphi_0, \varphi_1, \varphi_2 \ldots, \varphi_m) p^m \tag{38}$$

It is revealed that the convergence of Eq. (33) is a dependent of the auxiliary constants $C_1, C_2, \ldots$ at $p = 1$, one has;

$$\tilde{\varphi} = (t, C_1, \mathrm{C}_2, \ldots \mathrm{C}_m) = \varphi_0(t) + \sum_{j=1}^{m} \varphi_i(t, C_1, \mathrm{C}_2, \ldots \mathrm{C}_m) \tag{39}$$

Substitute Eq. (39) into Eq. (30) will give

$$R(t, C_1, \mathrm{C}_2, \ldots \mathrm{C}_m) = L(\tilde{\varphi}(t, C_1, \mathrm{C}_2, \ldots \mathrm{C}_m)) + g(t) + N(\tilde{\varphi}(t, C_1, \mathrm{C}_2, \ldots \mathrm{C}_m)) \tag{40}$$

If $R = 0$ then $\tilde{\varphi}$ will be the exact solution. There are many methods of residuals to find the optimal value $C_i, i = 1, 2, 3, \ldots m$. We may apply the least-squares method.

$$J(\mathrm{C}_1, \mathrm{C}_2, \ldots, \mathrm{C}_m) = \int_a^b R^2(t, \mathrm{C}_1, \mathrm{C}_2, \ldots, \mathrm{C}_m) dt \tag{41}$$

where R is residual and;

$$R = L(\tilde{\varphi}) + \mathrm{g}(t) + N(\tilde{\varphi}) \tag{42}$$

Also

$$\frac{\partial J}{\partial C_1} = \frac{\partial J}{\partial C_2} = \ldots = \frac{\partial J}{\partial C_m} = 0, \tag{43}$$

where a and b are properly chosen numbers to locate the desired $C_i, i = 1, 2, 3, \ldots m$

3.1.3 Application of the OHAM

Considering the following Duffing equation

$$\ddot{\varphi}_s(t) + \zeta \dot{\varphi}_s(t) + \omega_0^2 \varphi_s(t) + \mu \varphi_s^3(t) = \mathrm{Q} \cos \Omega t, \qquad \varphi_s(0) = A, \ \dot{\varphi}_s(0) = 0, \tag{44}$$

We can construct an OHAM in this form;

$$(1-p)\left[\ddot{\varphi}_s(t) + \omega_0^2 \varphi_s(t) \right] = H(t, p)\left[\ddot{\varphi}_s(t) + \omega_0^2 \varphi_s(t) + \zeta \dot{\varphi}_s(t) + \mu \varphi_s^3(t) - \mathrm{Q} \cos \Omega t \right],$$
$$\varphi_s(0, p) = A, \ \dot{\varphi}_s(t, p) = 0, \qquad p \in [0, 1]. \tag{45}$$

where ζ is the damping coefficient, μ is the cubic nonlinearity, Ω is the exciting frequency and $\omega_0^2 = K/M$ which is the natural frequency, a is the amplitude of vibration. For primary resonance, the exciting frequency Ω is presumed to be close to ω_0 is a non-zero auxiliary function for $p \neq 0$.

The solution can be expanded in a series of;

$$\begin{aligned} &H(t,p) = pc_1 + p^2 c_2 \\ &\phi(t,p,\mathrm{C}_i) = \varphi_0(t) + \sum_{k\geq 1}^{\infty} \varphi_k(t,\mathrm{C}_i) p^k, \quad i = 1,2,\ldots \end{aligned} \tag{46}$$

Generally, one iteration cannot be done due to the complicated nonlinear equation. Therefore, an additional iteration method is needed. As such, the natural frequency ω is beneficial. Using the parameter p the succeeding equation is obtained.

$$\Omega^2 = \omega_0^2(1 + p\sigma_1 + p^2\sigma_2 + p^3\sigma_3 \cdots), \tag{47}$$

where Ω is the approximate nonlinear frequency ω_0 is the linear natural frequency and σ_j are unknowns arriving from by removing the secularity conditions due to inhomogeneity in the expression [31].

$$\omega_N^2 = \lim_{p\to 0=1} = \Omega^2 = \omega_0^2(1 + \sigma_1 + \sigma_2 + \sigma_3 \cdots), \tag{48}$$

The expansion is like the Lindstedt-Poincaré method, we introduce a new variable τ the unknown period T.

$$\tau = \Omega t, \qquad \tau = \frac{2\pi t}{T}, \tag{49}$$

where ω is the natural frequency. Then Eq. (51) can be rephrased as:

$$\Omega^2 \ddot{\varphi}_s(\tau) + \omega_0^2 \varphi_s(\tau) = p(\mathrm{Q}\cos\Omega\tau - \zeta\,\Omega\dot{\varphi}_s(\tau) - \mu\varphi_s^3(\tau)), \tag{50}$$

Then substituting Eq. (46) and Eq. (47) into (45), and equating terms of identical powers of p, yields the following equations.

Zeroth Order of

$$p^0 : \frac{d^2\varphi_0}{d\tau^2} + \varphi_0 = 0, \qquad \varphi(0) = A, \qquad \dot{\varphi}(0) = 0, \tag{51}$$

First Order

$$p^1 : \frac{d^2\varphi_1}{d\tau^2} + \varphi_1 = -c_1\left(\frac{d^2\varphi_0}{d\tau^2} + \varphi_0 + \zeta\frac{d\varphi_0}{d\tau} + \frac{\mu}{\omega_0^2}\varphi_0^3 - \frac{Q}{\omega_0^2}\cos(\tau)\right) - \sigma_1\frac{d^2\varphi_0}{d\tau^2} + \frac{d^2\varphi_0}{d\tau^2} + \varphi_0, \qquad \varphi(0) = 0, \qquad \dot{\varphi}(0) = 0, \tag{52}$$

Second-Order

$$\begin{aligned} p^2 : \frac{d^2\varphi_2}{d\tau^2} + \varphi_2 = &-c_2\left(\frac{d^2\varphi_0}{d\tau^2} + \varphi_0 + \zeta\frac{d\varphi_0}{d\tau} + \frac{\mu}{\omega_0^2}\varphi_0^3 - \frac{Q}{\omega_0^2}\cos(\tau)\right) - \sigma_1\frac{d^2\varphi_1}{d\tau^2} - \sigma_2\frac{d^2\varphi_0}{d\tau^2} + \varphi_1 \\ &-c_1\left(\frac{d^2\varphi_1}{d\tau^2} + \sigma_1\frac{d^2\varphi_0}{d\tau^2} + \varphi_1 + \zeta\frac{d\varphi_1}{d\tau} + \sigma_1\zeta\frac{d\varphi_0}{d\tau} + 3\frac{\mu}{\omega_0^2}\varphi_0^2\varphi_1\right) + \frac{d^2\varphi_1}{d\tau^2} + \sigma_1\frac{d^2\varphi_0}{d\tau^2}, \\ &\varphi(0) = 0, \qquad \dot{\varphi}(0) = 0, \end{aligned} \tag{53}$$

Solving Eq. (51) along with the conditions, we have

$$\varphi_0 = A\cos(\tau), \tag{54}$$

Substitute Eq. (54) into Eq. (52), we have

$$\frac{d^2\varphi_1}{d\tau^2} + \varphi_1 = Ac_1\left(\frac{\sigma_1}{c_1} - \frac{3A^2}{4}\frac{\mu}{\omega_0^2} + \frac{Q}{A\omega_0^2}\right)\cos(\tau) + \sigma_1\zeta A\sin(\tau) - \frac{A^3}{4}\frac{c_1\mu}{\omega_0^2}\cos 3\tau, \tag{55}$$

To eradicate the secular terms, the following should be satisfied

$$\begin{aligned} &\sigma_1\zeta A = 0, \\ &Ac_1\left(\frac{\sigma_1}{c_1} - \frac{3A^2}{4}\frac{\mu}{\omega_0^2} + \frac{Q}{A\omega_0^2}\right) = 0, \end{aligned} \tag{56}$$

Therefore

$$\frac{\sigma_1}{c_1} = \frac{3A^2}{4}\frac{\mu}{\omega_0^2} - \frac{Q}{A\omega_0^2} \tag{57}$$

A particular solution of Eq. (55) is

$$\begin{aligned} &\frac{d^2\varphi_1}{d\tau^2} + \varphi_1 = -\frac{A^3}{4}\frac{c_1\mu}{\omega_0^2}\cos 3\tau, \\ &\varphi_1 = -\frac{A^3}{32}\frac{c_1\mu}{\omega_0^2}\cos\tau + \frac{A^3}{32}\frac{c_1\mu}{\omega_0^2}\cos 3\tau, \end{aligned} \tag{58}$$

Substituting $\sigma_1, \varphi_0, \varphi_1$ and into Eq. (53) one gets further iterations.

$$\begin{aligned} \frac{d^2\varphi_2}{d\tau^2} + \varphi_2 = {} & A\left(c_2\zeta + c_1\sigma_1\zeta - \frac{A^2}{32}\frac{\zeta c_1^2\mu}{\omega_0^2}\right)\sin(\tau) + \\ & A\left(\frac{c_2Q}{A\omega_0^2} - \frac{3A^2}{4}\frac{c_2\mu}{\omega_0^2} + \frac{9c_1\mu^2A^4}{32} + c_1\sigma_1 - \frac{A^2\mu\sigma_1}{32}\frac{c_1}{\omega_0^2} + \sigma_2 - \sigma_1\right)\cos(\tau) + \\ & A\left(\frac{A^2}{4}\frac{c_1^2\mu}{\omega_0^2} - \frac{A^2}{4}\frac{c_2\mu}{\omega_0^2} + \frac{9A^2}{32}\frac{\sigma_1c_1\mu}{\omega_0^2} - \frac{A^2}{4}\frac{c_1\mu}{\omega_0^2} + \frac{15c_1\mu^2A^4}{128} - \frac{3A^5c_1^2\mu^2}{32}\right)\cos(3\tau) + \\ & -\frac{3A^3}{32}\frac{c_1^2\mu}{\omega_0^2}\sin(3\tau) + \frac{3A^5c_1\mu^2}{128}\cos(5\tau), \end{aligned} \tag{59}$$

To eliminate the secular terms, the following should be satisfied

$$\begin{aligned} &A\left(c_2\zeta + c_1\sigma_1\zeta - \frac{A^2}{32}\frac{\zeta c_1^2\mu}{\omega_0^2}\right) = 0, \\ &A\left(\frac{c_2Q}{A\omega_0^2} - \frac{3A^2}{4}\frac{c_2\mu}{\omega_0^2} + \frac{9c_1\mu^2A^4}{32} + c_1\sigma_1 - \frac{A^2\mu\sigma_1}{32}\frac{c_1}{\omega_0^2} + \sigma_2 - \sigma_1\right) = 0, \end{aligned} \tag{60}$$

Therefore

$$\sigma_2 = \frac{3A^2}{4}\frac{c_2\mu}{\omega_0^2} - \frac{c_2 Q}{A\omega_0^2} - c_1\sigma_1 - \frac{9c_1\mu^2A^4}{32} + \frac{A^2\mu\sigma_1}{32}\frac{c_1}{\omega_0^2} + \sigma_1, \tag{61}$$

A particular solution of Eq. (59) is

$$\begin{aligned}
&\frac{d^2\varphi_2}{d\tau^2} + \varphi_2 = A\left(\frac{A^2}{4}\frac{c_1^2\mu}{\omega_0^2} - \frac{A^2}{4}\frac{c_2\mu}{\omega_0^2} + \frac{9A^2}{32}\frac{\sigma_1 c_1\mu}{\omega_0^2} - \frac{A^2}{4}\frac{c_1\mu}{\omega_0^2} + \frac{15c_1\mu^2A^4}{128} - \frac{3\mu^2A^4c_1^2}{32}\right)\cos(3\tau) \\
&\qquad - \frac{3A^3}{32}\frac{\zeta c_1^2\mu}{\omega_0^2}\sin(3\tau) + \frac{3A^5c_1^2\mu^2}{128}\cos(5\tau), \\
&\varphi_2 = \frac{9A^3\zeta c_1^2\mu}{256\omega_0^2}\sin(\tau) - \frac{\mu A^3\left(11A^2\mu c_1^2\omega_0^2 - 15A^2c_1\mu\omega_0^2 - 32c_1^2 - 36c_1\sigma_1 + 32c_1 + 32c_2\right)}{1024\omega_0^2}\cos(\tau) \\
&-\frac{\mu A^3}{64\omega_0^2}\left(\begin{array}{l} A^2\mu c_1^2\omega_0^2\left(\cos(\tau)\right)^5 + \left(\left(-\frac{17A^2\mu\omega_0^2}{4}+8\right)c_1^2 + \left(\frac{15A^2\mu\omega_0^2}{4}+9\sigma_1-8\right)c_1 - 8c_2\right)\left(\cos(\tau)\right)^3 \\ +3\sin(\tau)\left(\cos(\tau)\right)^2\zeta c_1^2 + \left(\left(\frac{41A^2\mu\omega_0^2}{16}-6\right)c_1^2 + \left(-\frac{45A^2\mu\omega_0^2}{16}-\frac{27\sigma_1}{4}+6\right)c_1 + 6c_2\right)\cos(\tau) \\ -\frac{3}{4}\sin(\tau)\zeta c_1^2 \end{array}\right),
\end{aligned} \tag{62}$$

Accordingly, the first order estimated solution of Eq. (46) is

$$\begin{aligned}
&\varphi = \lim_{p\to 1}(\varphi_0 + p\varphi_1) = \varphi_0 + \varphi_1 + \varphi_2, \\
&\varphi = A\cos(\tau) - \frac{A^3}{32}\frac{c_1\mu}{\omega_0^2}\cos\tau + \frac{A^3}{32}\frac{c_1\mu}{\omega_0^2}\cos 3\tau + \frac{9A^3\zeta c_1^2\mu}{256\omega_0^2}\sin(\tau) \\
&\quad - \frac{\mu A^3\left(11A^2\mu c_1^2\omega_0^2 - 15A^2c_1\mu\omega_0^2 - 32c_1^2 - 36c_1\sigma_1 + 32c_1 + 32c_2\right)}{1024\omega_0^2}\cos(\tau) \\
&-\frac{\mu A^3}{64\omega_0^2}\left(\begin{array}{l} A^2\mu c_1^2\omega_0^2\left(\cos(\tau)\right)^5 + \left(\left(-\frac{17A^2\mu\omega_0^2}{4}+8\right)c_1^2 + \left(\frac{15A^2\mu\omega_0^2}{4}+9\sigma_1-8\right)c_1 - 8c_2\right)\left(\cos(\tau)\right)^3 \\ +3\sin(\tau)\left(\cos(\tau)\right)^2\zeta c_1^2 + \left(\left(\frac{41A^2\mu\omega_0^2}{16}-6\right)c_1^2 + \left(-\frac{45A^2\mu\omega_0^2}{16}-\frac{27\sigma_1}{4}+6\right)c_1 + 6c_2\right)\cos(\tau) \\ -\frac{3}{4}\sin(\tau)\zeta c_1^2 \end{array}\right),
\end{aligned} \tag{63}$$

Also, applying Eq. (50), we have the first-order nonlinear frequency ratio

$$\begin{aligned}
&\frac{\omega_N^2}{\omega_0^2} = \lim_{p\to 0=1}\Omega^2 = (1 + \sigma_1 + \sigma_2\cdots), \\
&\sigma_1 = \sqrt{1 + \frac{3A^2c_1}{4}\frac{\mu}{\omega_0^2} - \frac{Qc_1}{A\omega_0^2} + \zeta A},
\end{aligned} \tag{64}$$

Substituting Eq. (63) into Eq. (46), we get the residual

$$R(t;\mathrm{C}_1,\mathrm{C}_2) = \frac{d^2\varphi}{d\tau^2} + \omega_0^2\varphi + \zeta\frac{d\varphi}{d\tau} + \mu\varphi_0^3 - \bar{Q}\cos(\tau), \tag{65}$$

where ϕ is Eq. (63). Therefore, the residual equal

$$R = \frac{A^3 c_1 \mu}{32\omega_0^2}\cos(\tau) - \frac{9A^3 c_1 \mu}{32\omega_0^2}\cos(3\tau) - A\cos(\tau) - \frac{9\zeta \mu A^3 c_1^2}{256\omega_0^2}\sin(\tau) + \frac{A^3\mu\left(11A^2\mu c_1^2\omega_0^2 - 15A^2 c_1 \mu\omega_0^2 - 32c_1^2 - 36c_1\sigma_1 + 32c_1 + 32c_2\right)}{1024\omega_0^2}\cos(\tau), \tag{66}$$

For C_1 and C_2 we minimize the function as follows:

$$J(\mathrm{C}_1, \mathrm{C}_2) = \int_0^1 (R(\tau, \mathrm{C}_1, \mathrm{C}_2))^2 d\tau, \tag{67}$$

$$J = \frac{5765c_1^4 c_2}{44204} - \frac{78c_1^2 c_2^2}{8412065} + \frac{15401c_1^3 c_2}{42111} + \frac{35c_1 c_2^2}{2691804} + \frac{621849187c_1}{7} - \frac{1919343c_2}{425} - \frac{183372578c_1^2}{3} - \frac{4553603c_1^3}{52} + \frac{102869c_1^2 c_2}{24028} - \frac{117514c_1 c_2}{18377} + \frac{c_1^{10} c_2}{502451754} - \frac{4c_1^9 c_2}{296546041} + \frac{c_1^8 c_2^2}{2916657961171} + \frac{5c_1^8 c_2}{773626016} - \frac{c_1^7 c_2^2}{537240477311} + \frac{c_1^6 c_2^3}{31703948106480621} + \frac{17c_1^7 c_2}{147479304} - \frac{c_1^6 c_2^2}{2498433222532} - \frac{c_1^5 c_2^3}{7775879924812435}, \tag{68}$$

The unknown constant C_1 and C_2 can be determined by using the following conditions

$$\frac{\partial J}{\partial \mathrm{C}_1} = \frac{\partial J}{\partial \mathrm{C}_2} = 0, \tag{69}$$

We obtained,

$$\mathrm{C}_1 = 2.4025\times10^{-9}, \mathrm{C}_2 = 5.271143\times10^{6}, \tag{70}$$

4 RESULTS

The problem titled nonlinear investigation of non-homogeneous varying thickness circular plates resting on three-parameter elastic foundations under the impact of the magnetic field is investigated and the solutions are validated with results reported in cited literature Haterbouch and Benamar [32] to show the reliability and efficiency of OHAM. The circular plate material non-homogeneity is presumed to arise because of the parabolic and linear variation in Young's modulus likewise the density along the radial direction. Non-uniform thickness circular plate of the following material properties is considered:

Young modulus of $E = 210GPa$, material density $\rho = 7850kg/m^3$, the circular plate radius is considered to be 1m, the initial thickness of $h = 0.03m$, Poisson's ratio $\upsilon = 0.3$, a small external force $Q_0 = 1.5\times10^{-9}N/m^2$ is considered and the external magnetic field amplitude adopted is $B_{0z} = 400A/m$. Validation of the solution is presented in Table 1. A comparison study was done for a uniform thickness clamped edge isotropic circular plate, the investigation revealed that the proposed results are in good harmony with values presented by [32], maximum of 0.51% discrepancy is observed. Table 2 shows the comparison of the solutions obtained with OHAM with numerical using the Runge-Kutta method. An almost identical result is observed. The computational time for different values of amplitude along with the constant values of *C*'s is displayed in Table 3.

Table 1
Frequency ratio for a uniform thickness clamped edge isotropic circular plate of different values of non-dimensional vibration amplitudes.

W_{max}/h	[32]	Present study	% Variation
0.2	1.0072	1.007	0.02
0.4	1.0284	1.0238	0.46
0.5	1.0439	1.0414	0.25
0.6	1.0623	1.0597	0.26
0.8	1.1073	1.1049	0.24
1	1.1615	1.1564	0.51

Table 2
Deflection verification for large amplitude vibration.

t	$A = 1$			$A = 2$			$A = 4$		
	RK4	OHAM	Relative error	RK4	OHAM	Relative error	RK4	OHAM	Relative error
0	1.00000	1.00000	0.0000	2.00000	2.00000	0.0000	4.00000	4.00000	0.00000
1	-0.07960	-0.07970	0.0001	-0.12800	-0.12900	0.0010	0.22302	0.22350	0.00048
2	0.00660	0.00660	0.0000	0.01040	0.01040	0.0000	-0.01865	-0.01860	0.00005
3	-0.00040	-0.00040	0.0000	-0.00070	-0.00060	0.0001	0.00172	0.00170	0.00002
4	0.00020	0.00025	0.0001	0.00020	0.00020	0.0000	-0.00002	-0.00001	0.00001
5	0.00000	0.00000	0.0000	-0.00010	-0.00011	0.0000	-0.00004	-0.00005	0.00001
6	-0.00020	-0.00060	0.0004	-0.00020	-0.00020	0.0000	-0.00016	-0.00020	0.00004
7	-0.00010	-0.00010	0.0000	-0.00010	-0.00010	0.0000	-0.00012	-0.00010	0.00002
8	0.00000	0.00000	0.0000	0.00000	0.00003	0.0000	0.00002	0.00000	0.00002
9	0.00010	0.00010	0.0000	0.00010	0.00020	0.0001	0.00015	0.00010	0.00005
10	0.00010	0.00030	0.0002	0.00010	0.00010	0.0000	0.00014	0.00030	0.00016
11	0.00000	0.00000	0.0000	0.00000	0.00001	0.0000	0.00000	0.00000	0.00000
12	-0.00010	-0.00010	0.0000	-0.00010	-0.00010	0.0000	-0.00014	-0.00010	0.00004
13	-0.00010	-0.00020	0.0001	-0.00010	-0.00020	0.0001	-0.00015	-0.00010	0.00005
14	0.00000	0.00000	0.0000	0.00000	0.00000	0.0000	-0.00002	0.00000	0.00002
15	0.00010	0.00010	0.0000	0.00010	0.00010	0.0000	0.00012	0.00010	0.00002
16	0.00020	0.00020	0.0000	0.00020	0.00050	0.0003	0.00016	0.00020	0.00004
17	0.00000	0.00001	0.0000	0.00000	0.00000	0.0000	0.00005	0.00000	0.00005
18	-0.00010	-0.00010	0.0000	-0.00010	-0.00010	0.0000	-0.00011	-0.00010	0.00001
19	-0.00020	-0.00030	0.0001	-0.00020	-0.00030	0.0001	-0.00016	-0.00020	0.00004
20	-0.00010	-0.00010	0.0000	-0.00010	-0.00010	0.0000	-0.00007	-0.00010	0.00003

Table 3
Showing the Coefficient of C_1 and C_2 given by OHAM for different values of a with computation time.

A	C_1	C_2	Computational time (sec)
0.10	2.40E-09	5.27E+06	80.43
0.20	-9.11E-09	6.64E+05	35.98
0.30	-3.59E-09	1.98E+05	30.57
0.40	1.13E-08	8.43E+04	32.21
0.50	-3.52E-09	4.35E+04	32.73
0.60	5.10E-09	2.53E+04	36.14
0.80	2.15E-01	2.37E+05	122.2
1.00	7.17E-09	5.63E+03	39.01
2.00	-2.37E+00	-5.11E+07	98.93
4.00	2.47E-08	1.08E+02	123.93

4.1 Effect of foundation parameters

To study the effect of elastic foundations k_p, k_s and k_w on the circular plate behaviour, the nonlinear analysis is carried out and the obtained results are illustrated in Figs.8-15. The influence of the elastic foundations' variation on the amplitude with the nonlinear natural frequency is scrutinized and shown in Figs.8, 9, 12-14. From the results, hardening nonlinearity is observed. The nonlinear frequency increases as the stiffness values of the three parameters

foundation increases. This finding is in line with the observation made by Dumir [17]. However, for linear Winkler foundation Fig. 12, the nonlinear frequency decreases as the values of the foundation stiffness increases. Increase of foundation stiffness, the plate vibration deflection tends

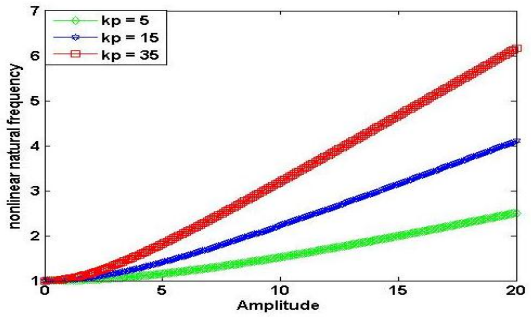

Fig.8
Influence of nonlinear Winkler foundation stiffness variation on the amplitude of vibration of linear varying parameters circular plate.

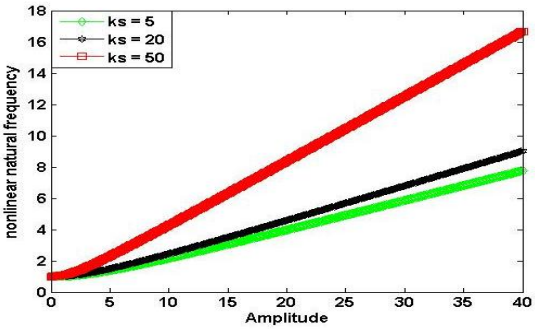

Fig.9
Influence of Pasternak foundation stiffness variation on the amplitude of vibration of linear varying parameters circular plate.

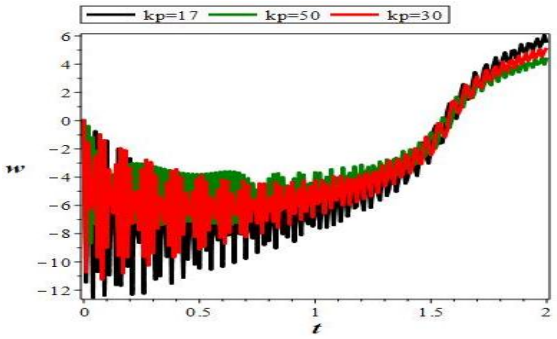

Fig.10
Influence of nonlinear Winkler foundation stiffness variation on deflection of linear varying thickness circular plate.

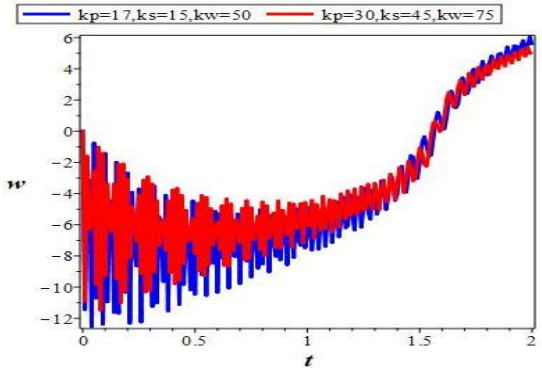

Fig.11
Influence of combined foundation stiffness variation on the deflection of linear varying thickness circular plate.

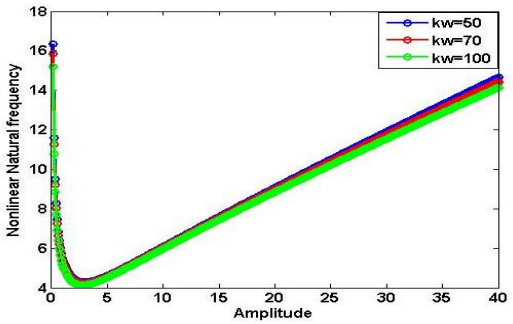

Fig.12
Influence of Winkler foundation stiffness variation on the amplitude of vibration for circular parabolic parameters variation plate.

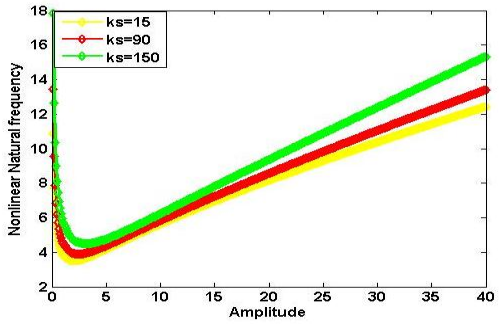

Fig.13
Influence of Pasternak foundation stiffness variation on the amplitude of vibration for circular parabolic plate.

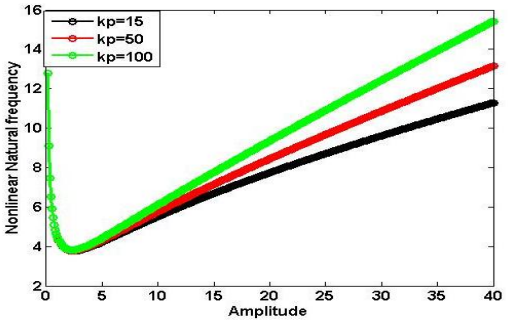

Fig.14
Influence of nonlinear Winkler foundation stiffness variation on the amplitude of vibration for circular parabolic plate.

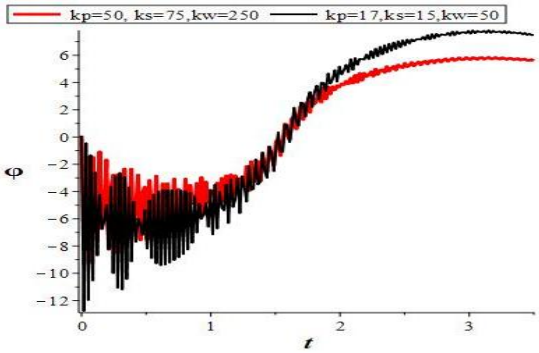

Fig.15
Influence of combined foundation stiffness variation on the deflection of parabolic varying thickness circular plate.

This can serve as the controlling parameter to the model nonlinearity. Figs. 10,11 and 15 show that the circular plate deflection decreases with an increase in nonlinear foundation parameters. This may be attributed to the fact that, as the shear stiffness of the foundation increases, this makes the plate stronger resulting in attenuation of the deflection Civalek [33].

4.2 Primary resonance response

To further analyze the influence of primary resonance on the parabolic and linear varying thickness with non-homogenous plate, the partial differential governing equations are transformed into the nonlinear ordinary equation through the Galerkin method. Subsequently, the Duffing equation obtained is analyzed using OHAM, and results are presented in Fig.16 and 17. The results further show that the nonlinear natural frequency is a function of amplitude. Increasing the forcing term increase the circular plate vibration amplitude.

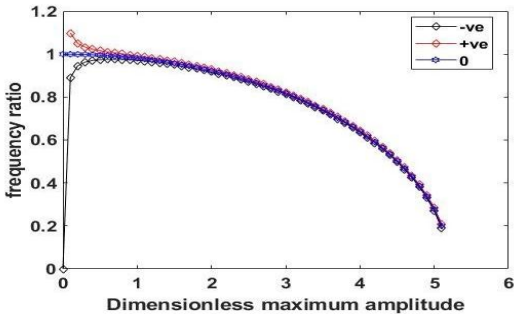

Fig.16
Influence of varying vibration amplitude on the nonlinear frequency-amplitude response curves for linear variation of parameters.

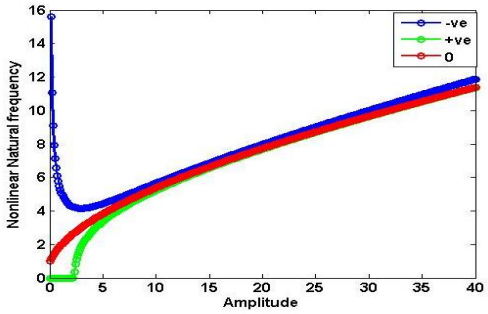

Fig.17
Influence of varying vibration amplitude on the nonlinear frequency-amplitude response curves for parabolic variation of parameters.

4.3 Effect of the magnetic field

The magnetic field influence is presented in Figs. 18, 19, 22, and 23. Based on the finding illustrated in Figs. 18 and 22, as the magnetic parameter increases, the deflection on the plate decreases. Attenuation of the deflection means that the magnetic field acts like a damper to the system which further prevents damage in the system as a direct result of vibration. Fig. 19 depicts that, the more the magnetic induction intensity is, the lower the nonlinear amplitude response of the circular plate linear varying thickness. Hu and Wang [34]. However, the result illustrated in Fig. 23 for parabolic varying parameters circular plate shows a contrary response to linear variation parameters. The nonlinear frequency increases as the values of the magnetic parameter increases.

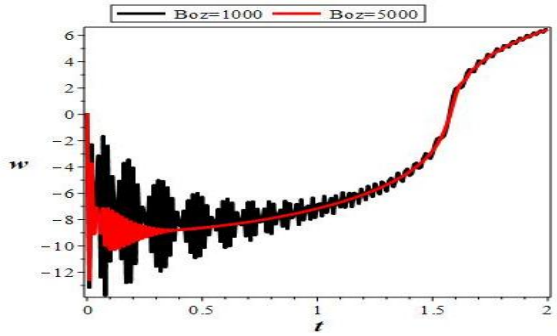

Fig.18
Effect of circular plate magnetic field deflection of linear varying thickness.

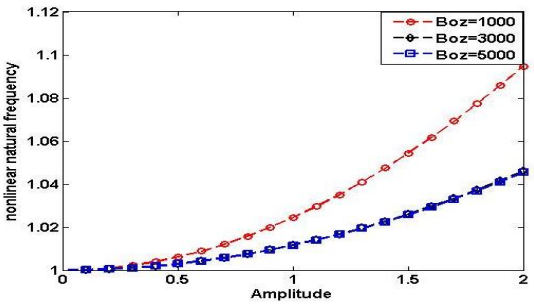

Fig.19
Effect of circular plate magnetic field on frequency-amplitude response curves of linear varying thickness.

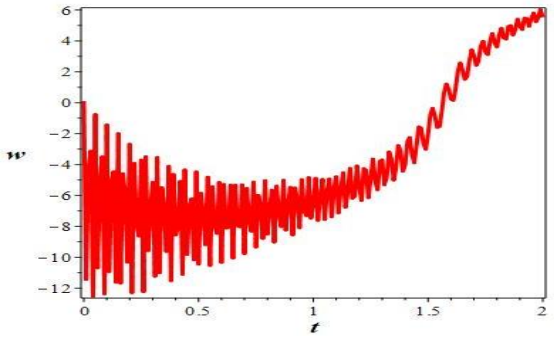

Fig.20
Circular plate midpoint deflection time history of linear varying thickness.

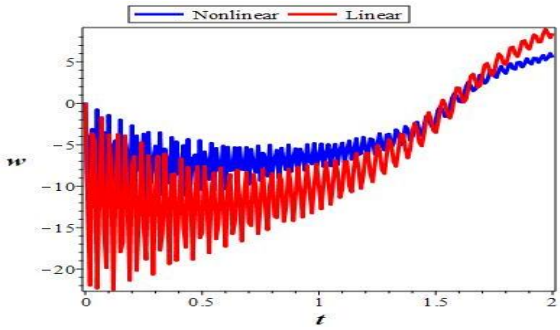

Fig.21
Circular plate midpoint deflection time history **c**omparison of the linear and nonlinear analysis of linear varying thickness.

Figs. 20 and 24 illustrate the nonlinear investigation of the midpoint time-deflection history of a circular plate of linear and parabolic thickness variation. While Figs. 21 and 25 show the assessment of linear with nonlinear vibration of the plate. It further shows from the diagram that, the nonlinear natural frequency is a function of amplitude, the higher the values of the amplitude the more pronounced is the variance between linear and nonlinear natural frequency.

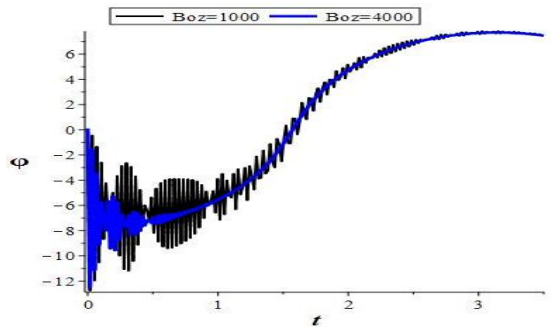

Fig.22
Effect of circular plate magnetic field deflection of parabolic varying thickness circular plate.

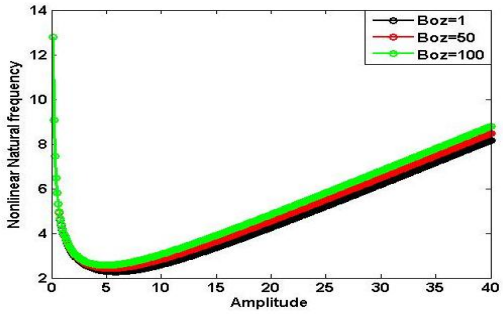

Fig.23
Effect of circular plate magnetic field on frequency-amplitude response curves of parabolic varying thickness.

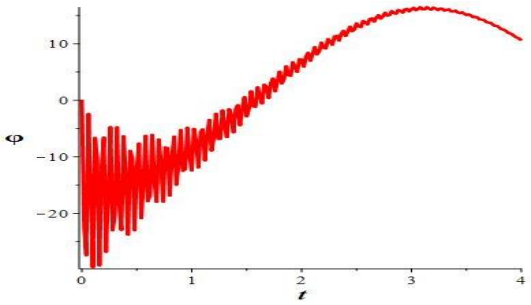

Fig.24
Circular plate midpoint deflection time history analysis of parabolic varying thickness.

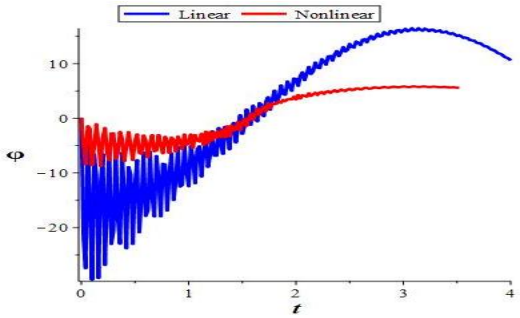

Fig.25
Circular plate midpoint deflection time history comparison of the linear and nonlinear analysis for parabolic varying thickness.

4.4 Influence of taper variation

Taper parameter variational influence on the nonlinear frequency response of the circular plate is studied and presented in Figs.26 and 28. In this analysis, homogeneity constant Young's modulus η and density α are taken as constant values respectively. Figs. 26 and 28 show taper parameter variational influence on the nonlinear frequency versus amplitude curve. It can be seen that; the nonlinear frequency of the varying thickness circular plate decreases with an increase in taper values. This is in harmony with [8,15] findings.

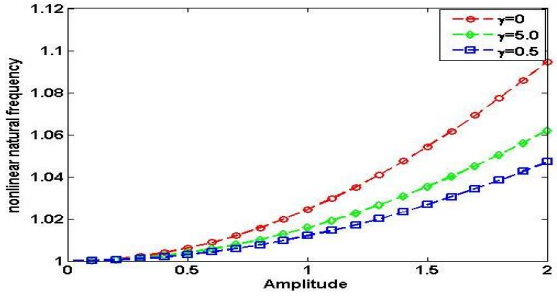

Fig.26
Influence of taper variation on the amplitude of vibration for linear varying parameters circular plate.

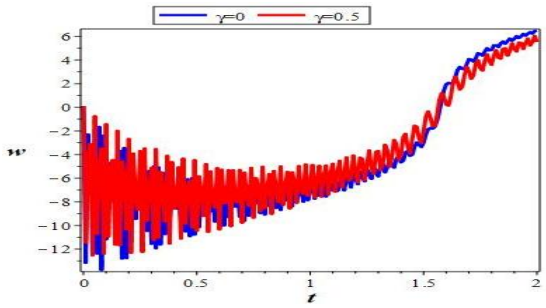

Fig.27
Influence of taper variation on circular plate maximum deflection of linear varying thickness.

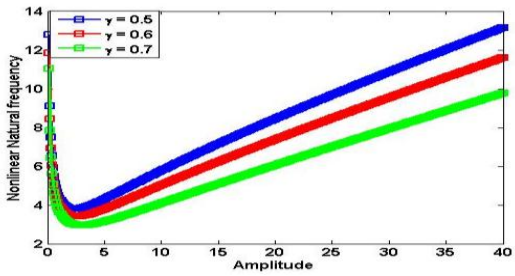

Fig.28
Influence of taper variation on the amplitude of vibration for parabolic varying parameters.

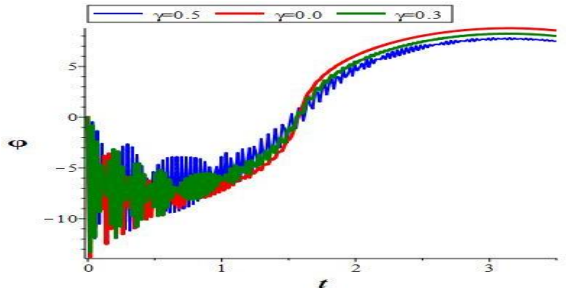

Fig.29
Influence of taper variation on circular plate maximum deflection of parabolic varying thickness.

while Figs.27 and 29 illustrate the attenuation of deflection due to an increase in the thickness of the circular plate. This is an obvious fact, the increase in stiffness of the plate, due to thickness increment lowers the deflection of the plate.

4.5 Effects of non-homogeneity variation

Figs.30-36 show the impact of circular plate non-homogeneity response of linear and parabolic varying thickness under magnetic field. This is obtained by linear and parabolic variation of the values of the density and Young's modulus of the circular plate. It is discovered that as the non-homogeneity values increases, the deflection of the circular plate decreases. Also, the nonlinear frequency of the varying thickness circular plate decreases with an increase in non-homogeneity values. The non-homogeneity being increase in flexural rigidity increases which leads to a decrease in the flexibility of the plate and consequently lowers the deflection [15].

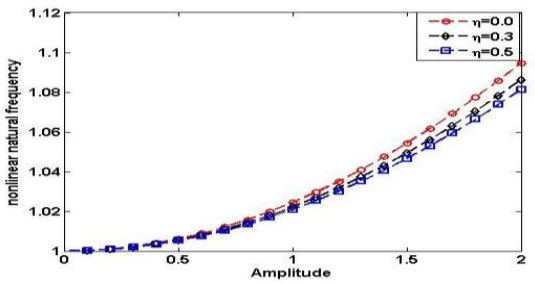

Fig.30
Influence of non-homogeneity variation on the amplitude of vibration for linear varying parameters circular plate.

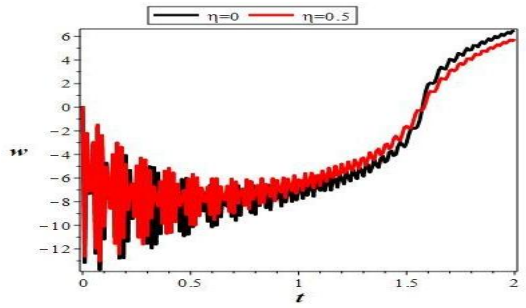

Fig.31
Influence of non-homogeneity variation on maximum deflection linear varying thickness.

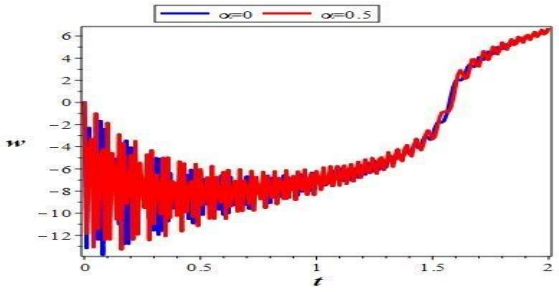

Fig.32
Influence of density variation on the maximum deflection of the linear varying thickness.

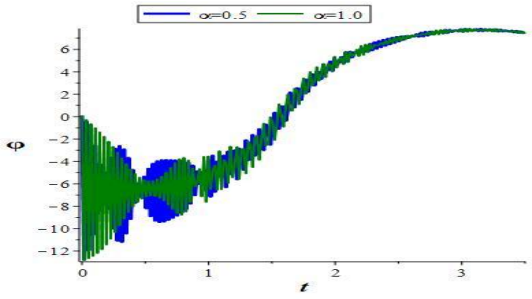

Fig.33
Influence of density variation on the maximum deflection of the parabolic varying thickness.

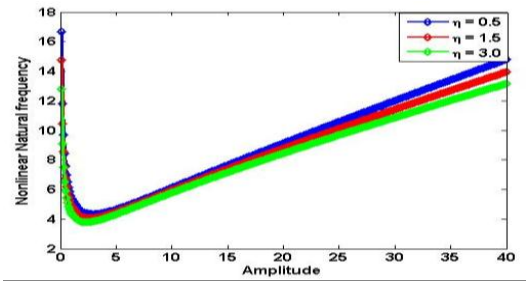

Fig.34
Influence of non-homogeneity variation on the amplitude of vibration for parabolic varying parameters.

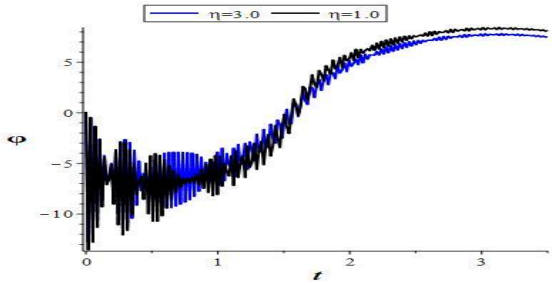

Fig.35
Influence of non-homogeneity variation on the maximum deflection of the parabolic varying thickness.

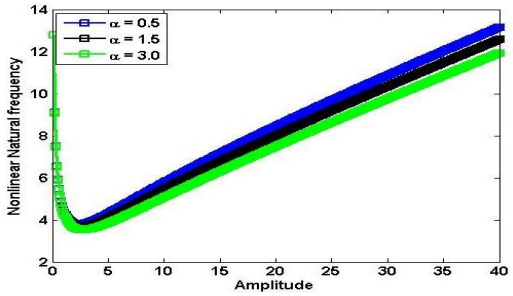

Fig.36
Influence of non-homogeneity variation on the amplitude of vibration for parabolic varying parameters.

4.6 Effect on boundary condition

To further study the influence of boundary conditions on the nonlinear frequency with amplitude, analysis is done, and the results are shown in Figs.37 and 38. It is clearly shown from the presented result that, vibration amplitude is lower for clamped edge condition than simply supported condition. The lower frequency ratio for clamped edge is a result of higher stiffness of the linear and parabolic varying thickness isotropic circular plate compared to simply supported condition.

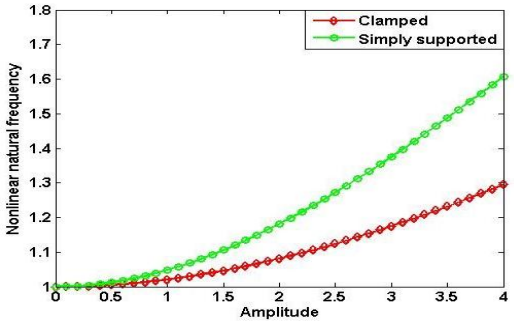

Fig.37
Influence of boundary conditions on circular plate nonlinear amplitude-frequency response curves of the linear varying parameters.

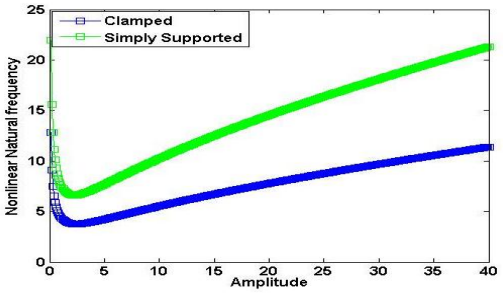

Fig.38
Influence of boundary conditions on isotropic circular plate nonlinear amplitude-frequency response curves of the parabolic varying parameters.

5 CONCLUSIONS

Nonlinear investigation of non-homogeneous varying thickness circular plates resting on three-parameter elastic foundations under the influence of the magnetic field is investigated. The nonlinear partial differential governing equation is transformed into the Duffing equation through the Galerkin method for transient state vibration analysis. The Ordinary differential equations were solved using Optimal Homotopy Asymptotic Method. The accuracies of the developed analytical solutions were verified with the results generated by some other methods as presented in the past works. The analytical solutions obtained were used to examine the effects of elastic foundations, boundary

conditions, non-homogeneity, thickness, and magnetic field on the dynamic response of the varying thickness circular plate. From the parametric studies, the following was observed:

1) Nonlinear frequency ratio increases with an increase in the linear elastic foundation. Pasternak parameter has a pronounced effect on the nonlinear frequency. Attenuation of maximum deflection occurs due to an increase in elastic foundation stiffness.
2) Maximum deflection and nonlinear frequency versus amplitude response decreases with increases in taper constant
3) Maximum deflection and nonlinear frequency versus amplitude response decrease as the non-homogeneity values increases.
4) The maximum deflection and nonlinear frequency versus amplitude response of the varying thickness circular plate decrease as the magnetic field parameters increases.
5) For primary resonance obtained, vibration amplitude is lower than the thickness of the plate and maximum amplitude occurs $Q = 0$.
6) Hardening nonlinearity is observed for both clamped and simply supported edge conditions. While the clamped edge has a lower amplitude.

From the present study, it can be concluded that OHAM is found to be powerful. More so, amazingly simple to apply when dealing with vibration plate involving variable thickness. The ability to correct the domain challenge is of immense benefit to the method. It is hoped that; these findings will add input to the existing fact in the dynamic theory of plate vibration.

ACKNOWLEDGMENTS

The authors acknowledge the support of the University of Lagos management and HERZER research group for providing the material supports for the research.

REFERENCES

[1] Zhiming Y., 1998, Nonlinear vibration of circular plate with exponential varying thickness, Journal of Shanghai University **2**(1): 27-33.
[2] Wattanasakulpong N., Charoensuk J., 2015, Vibration characteristics of stepped beams made of FGM using differential transform method, *Meccanica* **50**(4): 1089-1101.
[3] Chakravorty J.G., 1980, Bending of symmetrically loaded circular plate of variable thickness, *Indian Journal of Pure and Applied Mathematics* **11**(2): 258-267.
[4] Hu Y.D., Wang T., 2016, Nonlinear free vibration of a rotating circular plate under the static load in magnetic field, *Nonlinear Dynamics* **85**: 1825-1835.
[5] Wang C.M., Wang C.Y., Reddy J.N., 2004, *Exact Solution for Buckling of Structural Members*, CRC Press.
[6] Shi-Chao Y., Lin-Quan Y., Bal-Jian T., 2017, A novel higher-order shear and normal deformable plate theory for the static-free vibration and buckling analysis of functionally graded plate, *Mathematical Problems in Engineering* Article **2017**: ID 6879508.
[7] Shishesaz M., Zakipour A., Jafarzadeh A., 2016, Magneto-elastic analysis of annular FGM plate based on classical plate theory using GDQ method, *Latin America Journal of Solids Structures* **13**(14): 2436-2462.
[8] Banerjee B., 1983, Large deflection of circular plates of variable thickness, *Journalof Solids and Structures* **19**(2): 179-182.
[9] Shariyat M., Jafari A.A., Alipour M.M., 2013, Investigation of the thickness variability and material heterogeneity effects for free vibration of the viscoelastic circular plates, *Acta Mechanica Solida Sinica* **26**(1): 83-98.
[10] Gupta U.S., Sharma S., Singhal P., 2014, Effect of two-parameter foundation on free transverse vibration of non-homogenous orthotropic rectangular plate of linearly varying thickness, *Journal of Engineering and Applied Science* **6**(2): 32-51.
[11] Malekzadeh P., 2019, Three-dimensional free vibration analysis of thick functionally graded plates on elastic foundation, *Composite structure* **89**(3): 367-373.
[12] Kamal K., Durvasula S., 1983, Bending of circular plate on elastic foundation, *Journal of Engineering Mechanics* **109**: 1293-1298.
[13] Yazdi A.A., 2013, Homotopy perturbation method for nonlinear vibration analysis of functionally graded plate, Journal of Vibration and Acoustic **135**(2): 021012.
[14] Shama S., Lai R., Singh N., 2015, Effects of non-homogeneity on asymmetric vibration of non-uniform circular plates, *Journal of Vibration and Control* **23**: 1635-1644.

[15] Gupta A.K., Kumar L., 2010, Vibration of non-homogeneous visco-elastic circular plate of linearly varying thickness in steady-state temperature field, *Journal of Theoretical and Applied Mechanics* **48**(1): 255-266.

[16] Math Y., Varma K.K., Mahrenholtz D., 1986, Nonlinear dynamic response of rectangular plates on linear elastic foundation, *Computers & Structures* **4**: 391-399.

[17] Dumir P.C., 1986, Non-Linear vibration and post-buckling of isotropic thin circular plates on elastic foundations, *Journal of Sound and Vibration* **107**(2): 253-263.

[18] Touzé C., Thomas O., Chaigne A., 2002, Asymmetric non-linear forced vibrations of free-edge circular plates, *Journal of Sound and Vibration* **258**(4): 649-676.

[19] Bhoyar S., Varghese V., Khalsa L., 2020, Thermoelastic large deflection bending analysis of elliptical plate resting on elastic foundations, *Waves in Random and Complex Media*, DOI:10.1080/17455030.2020.1822563.

[20] Bhad P., Varghese V., Khalsa L., 2017, A modified approach for the thermoelastic large deflection in the elliptical plate, *Archive of Applied Mechanics* **87**: 767-781.

[21] Dastjerdi Sh., Yazdanparast L., 2018, New method for large deflection analysis of an elliptic plate weakened by an eccentric circular hole, *Journal of Solid Mechanics* **10**(3): 561-570.

[22] Dastjerdi Sh., Jabbarzadeh M., 2016, Nonlocal bending analysis of bilayer annular/circular nano plates based on first order shear deformation theory, *Journal of Solid Mechanics* **8**(3): 645-661.

[23] Dastjerdi Sh., Jabbarzadeh M., 2016, Non-Local thermo-elastic buckling analysis of multi-layer annular/circular nano-plates based on first and third order shear deformation theories using DQ method, *Journal of Solid Mechanics* **8**(4): 859-874.

[24] Dastjerdi Sh., Jabbarzadeh M., Aliabadi S., 2016, Nonlinear static analysis of single layer annular/circular graphene sheets embedded in Winkler–Pasternak elastic matrix based on non-local theory of eringen, *Ain Shams Engineering Journal* **7**(2): 873-884.

[25] Dastjerdi Sh., Beni Y.T., 2019, A novel approach for nonlinear bending response of macro- and nanoplates with irregular variable thickness under nonuniform loading in thermal environment, *Mechanics Based Design of Structures and Machines* **47**(4): 453-478.

[26] Yazdi A.A., 2016, Assessment of homotopy perturbation method for study the forced nonlinear vibration of orthotropic circular plate on elastic foundation, *Latin America Journal of Solids and Structures* **13**(2): 243-256.

[27] Zhong X., Liao S., 2016, Analytic solutions of von karman plate under arbitrary uniform pressure(1): Equations in differential form, *Studies in Applied Mathematics* **138**(4): 10.1111

[28] Wu T.Y., Liu G.R., 2001, Free vibration analysis of circular plates with variable thickness by the generalized differential quadrature*, International Journal of Solids and Structures* **38**: 7967-7980.

[29] Herisanu N., Marinca V., Dordea T., Madescu G., 2008, A new analytical approach to nonlinear vibration of an electrical machine, *Proceedings of the Romanian Academy - Series A* **9**(3): 229-236.

[30] Vasile M., Nicolae H., 2011, *Nonlinear Dynamical Systems in Engineering*, New York, Springer-Verlag Berlin Heidelberg.

[31] Marinca V., Herisanu N., Nemes L., 2008, Optimal homotopy asymptotic method with application to thin-film flow, *Central European Journal of Physics* **6**(3): 648-653.

[32] Haterbouch M., Benamar R., 2003, The effects of large vibration amplitudes on the axisymmetric mode shapes and natural frequencies of clamped thin isotropic circular plates, part I: iterative and explicit analytical solution for nonlinear transverse vibrations, *Journal of Sound and Vibration* **265**: 123-154.

[33] Civalek O., 2007, Nonlinear analysis of thin rectangular plates on Winkler-Pasternak elastic foundations by DSC-HDQ Methods*, Applied Mathematical Modelling* **31**: 606-624.

[34] Hu Y., Wang T., 2015, Nonlinear resonance of the rotating circular plate under static loads in magnetic field, *Chinese Jornal of Mechanical Engineering* **28**: 1277-1284.